Distributed Formation Control Under Arbitrarily Changing Topology

Kaveh Fathian, Dmitrii I. Rachinskii, Tyler H. Summers, Mark W. Spong, Nicholas R. Gans

***Abstract*— The problem of controlling a group of agents to achieve a desired geometric formation is considered. We provide sufficient conditions under which agents autonomously achieve any feasible desired formation, while the sensing topology among them can change arbitrarily. The desired formation is defined in terms of inter-agent distances and angles. Agents do not need to have a common or global coordinate frame, and local relative position measurements of their neighbors suffices to achieve the desired formation. Stability analysis, illustrative examples, and simulation results are provided.**

***Index Terms*— Multi agent formation control, distributed control, changing topology, switching sensing graph.**

I. Introduction

Distributed formation control aims to achieve a desired geometric configuration of agents, where agents execute the assigned control laws independently. Distributed formation control has application in several areas. A few examples are ground and/or aerial vehicle formations [1]–[3] for search, rescue, or inspection missions, vehicle platooning and automated highway systems [4], [5], cooperative robot manipulation and assembly [6], and modular robotics self configurations [7].

In many scenarios, a centralized formation control strategy may not be possible, and agents should independently and without communicating with each other achieve a desired formation. Furthermore, often position measurements cannot be acquired in a common or global coordinate frame. For example, in environments such as indoors, underwater, and space, GPS position measurements are not available. Distributed formation control techniques can be applied in such scenarios, and unlike centralized methods, have better scalability, naturally parallelized computation, resilience to communication loss and hardware failure, and robustness to uncertainty and lack of global knowledge.

The sensing topology among the agents is another factor that can make the formation control more challenging. In a dynamic sensing topology, the agents can lose or acquire sensing capability of other agents. For example, if a vision sensor is used to provide position measurements, sensing capability is lost when a neighbor agent is obstructed by another agent, and acquired when an agent moves in the line of sight. The changes in topology can be both temporal and spatial, and ideally the desired formation should be achieved regardless of how the topology changes.

*This work was supported by the OSD sponsored Autonomy Research Pilot Initiative project entitled A Privileged Sensing Framework, and the NSF grant DMS-1413223.

K. Fathian, M. W. Spong, and N. R. Gans are with the Department of Electrical Engineering, T. H. Summers is with the Department of Mechanical Engineering, D. I. Rachinskii is with the Department of Mathematical Sciences, University of Texas at Dallas, Richardson, TX, 75080 USA. E-mail: {kaveh.fathian, dmitry.rachinskiy, tyler.summers, mspong, ngans}@utdallas.edu.

Based on the definition of the desired formation, the existing literature on distributed formation control can be divided into distance-based [8]–[10], angle-based [11]–[14], or distance-angle based formations [15]–[19]. In distance-based and angle-based formations, the desired formation is defined in terms of inter-agent ranges and bearing angles, respectively. In distance-angle based formations, the desired formation is defined in terms of *both* parameters. This is because sensors that are used in practice such as ladar, radar, sonar, stereo cameras, etc., provide both angle and distance measurements, for which desired values can be defined. Our focus in this work is such desired formations.

In this work, we consider the distance-angle formation of a team of agents under an arbitrarily changing sensing topology. Inspired by the work in [20], [21], we use a linear control law for agents and present sufficient conditions under which the agents globally achieve the formation up to a scale factor. We then introduce a nonlinear term in the control law to fix the scale to a desired value. The convergence of the augmented control law is presented as a conjecture, however convergence to the desired shape is proven rigorously. Examples are provided throughout the paper to illustrate the concepts and control design, and simulations are presented to typify the performance.

The main contribution of this paper is a novel gain design technique that enables the agents to converge to a desired shape under an *arbitrarily* changing sensing topology. We are not aware of any previous work under this condition. In work where switching among topologies is considered [21], [22], typically the switches must satisfy a dwell time constraint or agents need to communicate. These constraints are not required in this work, and the topology can change arbitrarily fast. Furthermore, the control is distributed, only local relative position measurements are needed, local coordinate frames require no common orientation, and the convergence is global and has exponential rate.

The organization of the paper is as follows. The notation and assumptions are introduced in Section II. In Section III, the control law is formulated and preliminaries are discussed. In Section IV, the control gain design methodology is presented for both static and dynamic topologies, and the sufficient topological conditions for stability are derived. Proofs of the theorems and stability analysis are discussed in Section V. Lastly, in Section VI, simulation results for four agents with randomly changing sensing topology are presented.

II. Notation and Assumptions

We use the notation $\mathbb{N}_n := \{1, 2, ..., n\}$ to represent the set of natural numbers from 1 to n. The sensing topology among n agents is described by a directed graph $G = (\mathcal{V}, \mathcal{E})$, where $\mathcal{V} := \mathbb{N}_n$ is the set of vertices, and $\mathcal{E} \subset \mathcal{V} \times \mathcal{V}$ is the set of edges. Each vertex of the graph represents an agent. A directed edge from vertex $i \in \mathcal{V}$ to $j \in \mathcal{V}$ indicates that agent i can measure the relative position of agent j in its local coordinate frame. In such a case, agent j is called a neighbor of agent i. The set of neighbors of agent i is denoted by $\mathcal{N}_i := \{j \in \mathcal{V} \,|\, (i, j) \in \mathcal{E}\}$. An undirected edge between agent i and j in the graph indicates that they are both neighbors of each other.

We denote the distance between agent i and j by d_{ij}, and the desired distance by d^*_{ij}. If agent i has neighbors j and k, we denote by θ_{jik} the angle $\angle jik$, measured counterclockwise, and by θ^*_{jik} the desired angle. We say the desired *formation* is achieved if all distances and angles that agents make with their neighbors are the same as in the desired configuration. That is, for all $i \in \mathcal{V}$ and $j, k \in \mathcal{N}_i$, $d_{ij} = d^*_{ij}$ and $\theta_{jik} = \theta^*_{jik}$. We say the desired *shape* is achieved if only angles are the same as in the desired formation, i.e., the formation is achieved up to a (positive and possibly zero) scale factor. Throughout the paper the following assumptions hold.

Assumption 1. *The positions of all agents are restricted to a plane. Agents are numbered, i.e., they are distinguished, and know the identification number of their neighbors.*

Assumption 2. *Agents can measure the relative position of their neighbors in their local coordinate frames. They need not to have aligned or common coordinate frames, or communicate with other agents.*

Assumption 3. *The parameters that specify the desired formation are assumed to uniquely define a realizable formation (unique up to rotations and translations on the plane).*

Assumption 4. *The sensing topology should allow the desired formation to be realizable*[1] *(e.g., no disconnected graphs).*

Assumption 5. *Agents are treated as points on the plane, and collision avoidance is not considered.*

Assumption 6. *The agents have single-integrator holonomic dynamics*

$$\dot{x}_i = u_i, \tag{1}$$

where $x_i \in \mathbb{R}^2$ is the position vector of agent i, and $u_i \in \mathbb{R}^2$ is the control input to be determined.

III. Preliminaries

The materials presented in this section are based on the work in [21], where authors present the dynamics and control in the complex plane. We design the control and present the dynamics in $\mathbb{R}^2$.

[1]The necessary and sufficient topological conditions for realizability are discussed in [21], [23].

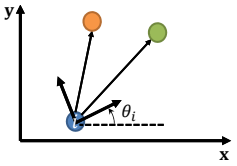

Fig. 1. Illustration of an agent with two neighbors. The local coordinate frame of agent i makes angle θ_i with the global coordinate frame (which is unknown to the agent).

Consider a team of n agents, and let $j \in \mathcal{N}_i$ be a neighbor of agent $i \in \mathbb{N}_n$. Let ${}^l x_j \in \mathbb{R}^2$ be the relative position of agent j in agent i's local coordinate frame. For simplicity, we can assume that the local coordinate frames are barycentric[2]. We use left superscript l to indicate that coordinates are in the local coordinate frames. Let $A_{ij} := \begin{bmatrix} a_{ij} & b_{ij} \\ c_{ij} & d_{ij} \end{bmatrix} \in \mathbb{R}^{2\times 2}$ be the matrix of control gains (to be designed). We define the control law for agent i in its local coordinate frame as

$${}^l u_i = \sum_{j \in \mathcal{N}_i} A_{ij} \, {}^l x_j. \tag{2}$$

Assume that the local coordinate frame of agent i makes angle θ_i with the global coordinate frame, as shown in Fig. 1. We will only use the global coordinates for stability analysis, and implementation of the control law (2) does not require the knowledge of global coordinates. If $R_{\theta_i} \in \mathrm{SO}(2)$ is the rotation matrix corresponding to θ_i, from (1) and (2) dynamics in the global coordinate frame are[3]

$$\begin{aligned} \dot{x}_i &= u_i \\ &= R_{\theta_i} \, {}^l u_i \\ &= \sum_{j \in \mathcal{N}_i} R_{\theta_i} A_{ij} \, {}^l x_j \\ &= \sum_{j \in \mathcal{N}_i} R_{\theta_i} A_{ij} R_{\theta_i}^{-1} (x_j - x_i). \end{aligned} \tag{3}$$

From (3), we observe that dynamics in the global coordinate frame generally depend on the orientations of the local coordinate frames (i.e., angles θ_i). However, if the rotation and gain matrices commute, (3) simplifies to

$$\begin{aligned} \dot{x}_i &= \sum_{j \in \mathcal{N}_i} A_{ij} R_{\theta_i} R_{\theta_i}^{-1} (x_j - x_i) \\ &= \sum_{j \in \mathcal{N}_i} A_{ij} (x_j - x_i), \end{aligned} \tag{4}$$

which is independent of the local coordinate frame orientations.

Lemma 1. *Control gain matrices A_{ij} that commute with rotation matrices R_{θ_i} are of the form*[4]

$$A_{ij} = \begin{bmatrix} a_{ij} & -b_{ij} \\ b_{ij} & a_{ij} \end{bmatrix}, \quad a_{ij}, b_{ij} \in \mathbb{R}. \tag{5}$$

[2]In a barycentric coordinate system, an agent is located at the origin of its local coordinate frame.

[3]Note that u_i is a vector, and its transformation from local to global coordinate frame or vice versa is independent of the translational difference between the coordinate frames.

[4]In the complex formulation discussed in [21], gains are represented by $z_{ij} := a_{ij} + \imath b_{ij}$, where $\imath$ is the imaginary unit.

The proof of Lemma 1 is trivial and not discussed here. By limiting the control gain matrix to the form (5), we can proceed by designing the control in the global coordinate frame, knowing that the local implementation (2) results in the same dynamics.

Let $x := [x_1^\top,\ x_2^\top,\ \ldots,\ x_n^\top]^\top \in \mathbb{R}^{2n}$ be the aggregate vector of agents' coordinates. Closed-loop dynamics (4) can be represented in the shorthand form

$$\dot{x} = Ax, \tag{6}$$

where $A \in \mathbb{R}^{2n\times 2n}$, and has block Laplacian structure. That is, for all $i \in \mathbb{N}_n$ and $j \in \mathcal{N}_i$, the 2×2 matrix block associated with rows $2i-1, 2i$ and columns $2i-1, 2i$ of A is $-\sum_{j\in\mathcal{N}_i} A_{ij}$, and the block associated with rows $2i-1, 2i$ and columns $2j-1, 2j$ is A_{ij}. The rest of the elements are zero (see Example 1).

Lemma 2. *Define vectors*

$$\begin{aligned}\mathbf{1} &:= [1, 1, \ldots, 1]^\top \in \mathbb{R}^{2n},\\ \bar{\mathbf{1}} &:= [-1,\ 1, -1,\ 1,\ \ldots, -1,\ 1]^\top \in \mathbb{R}^{2n}.\end{aligned} \tag{7}$$

From the block Laplacian structure of A together with control gain structure (5) *it follows that*

$$A\mathbf{1} = 0, \quad A\bar{\mathbf{1}} = 0. \tag{8}$$

Consider an arbitrary embedding of agents at their desired formation in the global coordinate frame. Let $x_i^* \in \mathbb{R}^2$ be the coordinates of agent i associated to this embedding. If the desired formation is an equilibrium of (4), at this embedding we should have $\dot{x}_i = 0$, and therefore

$$\sum_{j\in\mathcal{N}_i} A_{ij}(x_j^* - x_i^*) = 0, \quad \forall i \in \mathbb{N}_n. \tag{9}$$

Define the 90° rotated coordinates $\bar{x}_i^* := R_{\frac{\pi}{2}} x_i^*$ and the aggregate coordinate vectors

$$\begin{aligned}x^* &:= [x_1^{*\top},\ x_2^{*\top},\ \ldots,\ x_n^{*\top}]^\top \in \mathbb{R}^{2n},\\ \bar{x}^* &:= [\bar{x}_1^{*\top},\ \bar{x}_2^{*\top},\ \ldots,\ \bar{x}_n^{*\top}]^\top \in \mathbb{R}^{2n}.\end{aligned} \tag{10}$$

The following Lemma follows from (9) and the block Laplacian structure of A.

Lemma 3. *If x^* is an equilibrium of* (6)*, then the block Laplacian structure of A implies*

$$Ax^* = 0, \quad A\bar{x}^* = 0. \tag{11}$$

Proofs of Lemmas 2 and 3 are trivial and not discussed here. These Lemmas imply that A has four zero eigenvalues with corresponding eigenvectors $\mathbf{1}$, $\bar{\mathbf{1}}$, x^* and $\bar{x}^*$.

Example 1. Consider 3 agents with a complete sensing graph, i.e., each agent can sense the other two agents. Suppose that the desired formation is defined as a right triangle with side lengths $d_{32}^* = 3$, $d_{21}^* = 4$, and $d_{13}^* = 5$. An embedding of the agents at their desired formation is shown in Fig. 2, for which $x_1^* = [0,\ 0]^\top$, $x_2^* = [4,\ 0]^\top$ and $x_3^* = [4,\ 3]^\top$. Therefore

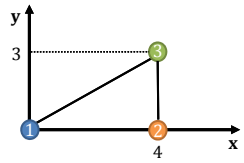

Fig. 2. An embedding of three agents at their desired formation.

$$x^* = \begin{bmatrix}0 & 0 & 4 & 0 & 4 & 3\end{bmatrix}^\top, \tag{12}$$

$$\bar{x}^* = \begin{bmatrix}0 & 0 & 0 & 4 & -3 & 4\end{bmatrix}^\top. \tag{13}$$

If the control gains are chosen as

$$\begin{aligned}A_{12} &= \frac{1}{3}\begin{bmatrix}3 & 4\\ -4 & 3\end{bmatrix}, \quad A_{13} = \frac{1}{3}\begin{bmatrix}0 & -4\\ 4 & 0\end{bmatrix},\\ A_{21} &= \frac{3}{25}\begin{bmatrix}3 & -4\\ 4 & 3\end{bmatrix}, \quad A_{23} = \frac{4}{25}\begin{bmatrix}4 & 3\\ -3 & 4\end{bmatrix},\\ A_{31} &= \frac{1}{4}\begin{bmatrix}0 & 3\\ -3 & 0\end{bmatrix}, \quad A_{32} = \frac{1}{4}\begin{bmatrix}4 & -3\\ 3 & 4\end{bmatrix},\end{aligned}$$

matrix A is given by

$$A = \begin{bmatrix}-1 & 0 & 1 & \frac{4}{3} & 0 & -\frac{4}{3}\\ 0 & -1 & -\frac{4}{3} & 1 & \frac{4}{3} & 0\\ \frac{9}{25} & -\frac{12}{25} & -1 & 0 & \frac{16}{25} & \frac{12}{25}\\ \frac{12}{25} & \frac{9}{25} & 0 & -1 & -\frac{12}{25} & \frac{16}{25}\\ 0 & \frac{3}{4} & 1 & -\frac{3}{4} & -1 & 0\\ -\frac{3}{4} & 0 & \frac{3}{4} & 1 & 0 & -1\end{bmatrix}.$$

One can verify that $A\mathbf{1} = A\bar{\mathbf{1}} = 0$, and $Ax^* = A\bar{x}^* = 0$.

IV. Main Results

We present the main contribution of the paper in this section, where we introduce a novel approach to design gain matrices A_{ij} of form (5), such that the desired *shape* is achieved under any arbitrarily switching topology. We first introduce the gain design methodology for a static sensing topology, and then extend it to dynamic sensing topologies. Lastly, we propose an augmented control law and conjecture that under this control agents achieve the desired *shape* and *scale*, i.e., the desired *formation*.

The analysis and proofs of the theorems presented in this section are presented in the next section. The following Lemma is well-known from linear systems theory.

Lemma 4. *If all nonzero eigenvalues of matrix A have negative real parts, then all trajectories of the linear dynamical system $\dot{x} = Ax$ exponentially converge to* $\ker(A)$[5].

Define

$$N := [\mathbf{1},\ \bar{\mathbf{1}},\ x^*,\ \bar{x}^*] \in \mathbb{R}^{2n\times 4}. \tag{14}$$

If A satisfies the conditions of Lemma 4, and $\ker(A) = \text{range}(N)$[6], then the desired formation is achieved

[5]If $A \in \mathbb{R}^{n\times n}$, kernel or null space of A is defined as $\ker(A) := \{v \in \mathbb{R}^n \,|\, Av = 0\}$.

[6]If $v_i \in \mathbb{R}^n$ is the i'th column of matrix $N \in \mathbb{R}^{n\times m}$, range or linear span of N is defined as $\text{range}(N) := \{\sum_{i=1}^m c_i v_i \,|\, c_i \in \mathbb{R}\}$.

up to scale factor. Note that in this case $\ker(A)$ is nothing but all rotations and translations of the desired shape.

A. Gain Design for Static Sensing Topology

We first present a method to find control gains a_{ij}, b_{ij}, such that for a fixed sensing topology, the agents converge to the desired shape. Let $USV^\top = N$ be the (full) singular value decomposition (SVD) of N, where

$$U = [\bar{Q},\ Q] \ \in \mathbb{R}^{2n\times 2n}, \tag{15}$$

with $Q \in \mathbb{R}^{2n\times(2n-4)}$ defined as the last $2n-4$ columns of U.

Lemma 5. *Using Q in* (15)*, define*

$$\bar{A} := Q^\top A Q \ \in \mathbb{R}^{(2n-4)\times(2n-4)}. \tag{16}$$

Matrices A and $\bar{A}$ have the same set of nonzero eigenvalues.

Proof of Lemma 5 follows by observing that U is an orthogonal matrix, and $\text{range}(\bar{Q}) = \text{range}(N)$. Therefore $\bar{A}$ is the projection of A onto the orthogonal complement of $\text{range}(N)$. Effectively, the projection (16) removes the zero eigenvalues of A and allows us to formulate the stability of A in terms of $\bar{A}$.

Example 2. Consider the 3 agent formation in Example 1. The eigenvalues of A are $\{0,0,0,0,-3,-3\}$. Substituting (12) and (13) in (14), SVD of N results in

$$Q^\top = \begin{bmatrix} 0.24 & -0.35 & -0.71 & 0.02 & 0.46 & 0.33 \\ 0.35 & 0.24 & -0.02 & -0.71 & -0.33 & 0.46 \end{bmatrix}, \tag{17}$$

where the entries in Q are rounded to two decimal digits. Thus

$$\bar{A} = Q^\top A Q = \begin{bmatrix} -3 & 0 \\ 0 & -3 \end{bmatrix},$$

from which one can see that nonzero eigenvalues of $\bar{A}$ and A are identical.

We denote the 2×2 matrix blocks in $\bar{A}$ by

$$\bar{A}_{rs} := \begin{bmatrix} \bar{a}_{2r-1\ 2s-1} & \bar{a}_{2r-1\ 2s} \\ \bar{a}_{2r\ 2s-1} & \bar{a}_{2r\ 2s} \end{bmatrix} \in \mathbb{R}^{2\times 2}, \quad r,s \in \mathbb{N}_{n-2}, \tag{18}$$

where $\bar{a}_{rs}$ represent the entries of $\bar{A}$.

Theorem 1. *Consider a team of n agents, and let $\varepsilon > 0$ be an arbitrary positive number. Let $r,s \in \mathbb{N}_{n-2}$. If control gains are chosen such that the constraints*

$$\begin{cases} \bar{A}_{rs} = 0, & \text{if } r < s \\ \text{diag}(\bar{A}_{rr}) \le -\varepsilon \\ Ax^* = 0 \end{cases} \tag{19}$$

are satisfied, under control (2)*, the agents converge to the desired shape from any starting configuration*[7].

Matrices $\bar{A}_{rs}, r < s$ are the 2×2 matrix blocks in $\bar{A}$ that are above the diagonal. Therefore, the first constraint in (19) implies that $\bar{A}$ is a block lower triangular matrix. The second constraint implies that all diagonal elements of $\bar{A}$ are negative, which is sufficient to ensure that $\bar{A}$ is stable[8]. The last constraint assures that the desired formation is an equilibrium (see proof of Theorem 1 for more detail).

We need to answer two questions. First, under what condition control gains exist that satisfy (19)? Second, if gains that satisfy (19) exist, how can they be found? To answer the first question, notice that (19) represents a system of *linear* constraints in terms of the control gains (see Example 3). Therefore, (19) generically has a solution when the number of constraints is less than or equal to the number of variables.

The total number of directed edges in the sensing graph is given by $\sum_{i=1}^{n} |\mathcal{N}_i|$, where $|\mathcal{N}_i|$ is the cardinality of $\mathcal{N}_i$. Note that the total number of directed edges in an undirected graph is twice the number of undirected edges. A directed edge between agents i and j corresponds to two control gains a_{ij}, b_{ij}. Thus, the total number of gains in a fixed sensing topology is given by

$$m := 2\sum_{i=1}^{n} |\mathcal{N}_i|. \tag{20}$$

Theorem 2. *Consider n agents with a fixed sensing topology, and m defined by* (20)*. If $m \ge (n-2)^2 + 2n$, the number of constraints in* (19) *is less than or equal to the number of control gains.*

To answer the second question, consider the optimization problem

$$\begin{aligned} \min_{a_{ij},b_{ij}} \quad & \sum_{r<s} \|\bar{A}_{rs}\|^2 \\ \text{subject to} \quad & \text{diag}(\bar{A}_{rr}) \le -\varepsilon \\ & Ax^* = 0 \end{aligned} \tag{21}$$

where $\|\bar{A}_{rs}\|$ denotes the Frobenius norm[9] of $\bar{A}_{rs}$, $r,s \in \mathbb{N}_{n-2}$, and $i,j \in \mathbb{N}_n$. The optimization (21) is a convex problem. Consequently, the minimum is well defined and the optimization algorithm converges to it from any starting point. Convex optimization solvers such as CVX [24] can be used to solve (21) efficiently.

By minimizing the cost function (21), we are trying to make $\bar{A}$ a block lower triangular matrix, and therefore satisfy the first constraint in (19). Since zero is the lower bound for the cost function, when (19) has a solution, gains found via (21) make $\bar{A}$ a stable block lower triangular matrix.

Example 3. Consider the 3 agent formation in Example 1, and suppose that the control gains are in the form (5) and need to be designed. The total number of control gains is $m = 12$, and $(n-2)^2 + 2n = 7$. Thus, conditions of Theorem 2 are met, and stabilizing gains are found via (21). Notice that for $n = 3$, $\bar{A}$ does not have any upper diagonal blocks, and therefore the cost function in (21) is identical to zero. Thus, the optimization reduces to finding the gains

[7] With a slight abuse of notation, $A = 0$ implies that all elements of matrix A are zero. Similarly, $\text{diag}(A) < -\varepsilon$ implies that each diagonal element of A is less than $-\varepsilon$.

[8] A stable or Hurwitz matrix is a matrix where the real part of its eigenvalues is negative.

[9] $\|\bar{A}_{rs}\|^2$ is the sum of squares of elements of $\bar{A}_{rs}$.

that satisfy the constraints. Using Q in (17), the constraint $\mathrm{diag}(\bar{A}_{11}) \leq -\varepsilon$ implies

$$\begin{aligned} 0.24b_{12} - 0.18a_{13} - 0.68a_{21} - 0.82a_{23} - 0.32a_{31} - 0.64a_{32} \\ -0.36a_{12} - 0.24b_{13} - 0.24b_{21} + 0.24b_{23} + 0.24b_{31} \\ -0.24b_{32} \leq -\varepsilon. \end{aligned}$$

The constraint $Ax^* = 0$ implies

$$\begin{aligned} 4a_{12} + 4a_{13} - 3b_{13} &= 0, \\ 3a_{13} + 4b_{12} + 4b_{13} &= 0, \\ -4a_{21} - 3b_{23} &= 0, \\ 3a_{23} - 4b_{21} &= 0, \\ 3b_{31} - 4a_{31} + 3b_{32} &= 0, \\ -3a_{31} - 3a_{32} - 4b_{31} &= 0, \end{aligned}$$

which is the same as $A\bar{x}^* = 0$. The total number of 7 linear constraints in 12 variables implies that there are infinitely many choices for the stabilizing gains. A possible set of gains were given in Example 1.

Remark 1. *It is possible to design stabilizing gains for static graphs that have fewer edges than the required number in Theorem 2. However, the advantage of formulation* (21) *is that it provides a straightforward way to find gains for dynamic topologies.*

Lastly, note that when the number of edges is smaller than the required number in Theorem 2, (21) *may* still result in a $\bar{A}$, which although not block lower triangular, is stable.

B. Gain Design for Dynamic Sensing Topology

We proceed by designing the gains for a dynamic sensing topology, such that the desired shape is achieved regardless of how the topology changes in time. To illustrate the difference in gain design between static and dynamic topologies, consider an example of four agents in Fig. 3, where all possible undirected topologies among the agents are numbered from 1 to 10. Recall that by assumption, the topology should allow the desired formation to be realizable, therefore, disconnected graphs and graphs in which an agent has only one neighbor are not considered.

Consider the first and second topologies in Fig. 3. Agents 2 and 3 have the same neighbor set in both topologies, i.e., $\mathcal{N}_2^1 = \mathcal{N}_2^2$ and $\mathcal{N}_3^1 = \mathcal{N}_3^2$, where we used right superscripts to distinguish the topologies. Unless additional information is provided to the agents, agents 2 and 3 cannot distinguish between the two topologies. Therefore, the same set of gains used for them in the first topology should work for the second topology. On the other hand, agents 1 and 4 have different neighbor sets. Therefore they can distinguish between topologies and possibly have different gains.

Theorem 3. *Let $\mathcal{G} := \{G^1, G^2, \ldots, G^K\}$ represent a finite set of K sensing topologies, where we use right superscripts to distinguish the topologies and their associated variables. Let $r,s \in \mathbb{N}_{n-2}$ and $k,l \in \mathbb{N}_K$. If control gains a_{ij}^k, b_{ij}^k, are chosen*

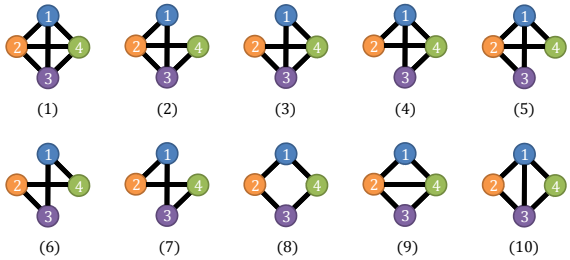

Fig. 3. All feasible undirected sensing topologies among 4 agents.

such that the constraints

$$\begin{cases} \bar{A}_{rs}^k = 0, & \text{if } r < s \\ \mathrm{diag}(\bar{A}_{rr}^k) \leq -\varepsilon & \\ A^k x^* = 0 & \\ a_{ij}^k = a_{ij}^l,\ b_{ij}^k = b_{ij}^l, & \text{if } \mathcal{N}_i^k = \mathcal{N}_i^l \end{cases} \tag{22}$$

are satisfied, using control (2)*, agents converge to the desired shape under any arbitrarily changing topology $G^{k(t)} \in \mathcal{G}$. Moreover, convergence rate is exponential.*

The first constraint in (22) implies that all $\bar{A}^k$ matrices are block lower triangular. The second constraint ensures that all matrices are stable. Convergence under arbitrarily switching among topologies is a consequence of this stable block lower triangular structure. The last constraint ensures that when an agent has the same neighbor set in two different topologies, its associated gains are identical.

Similar to the case for static topologies, we need to find out under what condition the number of constraints in (22) is less than or equal to the number of control gains. Define

$$s_i^k := \begin{cases} 0, & \text{if } \exists_{l<k} \text{ s.t. } \mathcal{N}_i^k = \mathcal{N}_i^l \\ 1, & \text{otherwise} \end{cases}, \tag{23}$$

to indicate if the neighbor set of agent i in topology G^k has been identical to its neighbor set in any previous topology G^l, $l < k$. Note that $\sum_{k=1}^K s_i^k$ shows the number of nonidentical neighbor sets of agent i in all topologies. Denote by

$$S = \sum_{i=1}^{n} \sum_{k=1}^{K} s_i^k, \tag{24}$$

the total number of nonidentical neighbor sets for all agents in all topologies. Further define the number of independent gains by

$$m := 2 \sum_{i=1}^{n} \sum_{k=1}^{K} s_i^k \, |\mathcal{N}_i^k|, \tag{25}$$

where $|\mathcal{N}_i^k|$ is the cardinality of $\mathcal{N}_i^k$. The number of independent gains, m, describes the number of available gains after enforcing the constraint $a_{ij}^k = a_{ij}^l$, $b_{ij}^k = b_{ij}^l$ if $\mathcal{N}_i^k = \mathcal{N}_i^l$. That is, the overall number of gains in all topologies, where gains for agents with identical neighbor sets are only counted once.

Theorem 4. *Consider n agents with a set $\mathcal{G}$ of K sensing topologies, and S and m defined by* (24) *and* (25)*. If $m \geq K(n-2)^2 + 2S$, then the number of constraints in* (22) *is less than or equal to the number of control gains.*

When conditions in Theorem 4 are met, simultaneously stabilizing gains can be found by solving the convex optimization problem

$$\begin{aligned} \min_{a_{ij}^k, b_{ij}^k} \quad & \sum_{k=1}^{K} \sum_{r<s} \|\bar{A}_{rs}^k\|^2 \\ \text{subject to} \quad & \operatorname{diag}(\bar{A}_{rr}^k) \leq -\varepsilon \\ & A^k x^* = 0 \\ & a_{ij}^k = a_{ij}^l,\ b_{ij}^k = b_{ij}^l \ \text{ if } \mathcal{N}_i^k = \mathcal{N}_i^l \end{aligned} \tag{26}$$

where $k,l \in \mathbb{N}_K$, $\varepsilon > 0$, $r,s \in \mathbb{N}_{n-2}$, and $i,j \in \mathbb{N}_n$.

For a given desired formation, the control gains are found via (26) prior to deployment. Each agent receives its associated gain set and is not aware of other agents' gains. At each instant of time, agents choose their control gains according to their current neighbor set.

C. Fixing the Scale

So far we have discussed how control gains can be designed such that under the control law (2), the agents achieve the desired shape, i.e., the desired formation up to a scale factor. To fix the scale, we propose the augmented control law

$${}^l u_i = \sum_{j \in \mathcal{N}_i} A_{ij}\ {}^l x_j + f(d_{ij} - d_{ij}^*)\ {}^l x_j, \tag{27}$$

where $d_{ij} := \|{}^l x_j\| = \|x_j - x_i\|$ denotes the distance between agent i and j, and $d_{ij}^* \in \mathbb{R}$ is its desired value that is given from the desired formation. Smooth map $f : \mathbb{R} \to \mathbb{R}$ is chosen such that for all $z \in \mathbb{R}$, $zf(z) > 0$ for $z \neq 0$, and $f(0) = 0$. Moreover f is bounded by $|f(z)| \leq f_{\max}, \forall_{z \in \mathbb{R}}$. Possible choices for f are $f : z \mapsto \frac{1}{c}\arctan(z)$ or $f : z \mapsto \frac{1}{c}\tanh(z)$, where $c > 0$ is an arbitrary constant that can be chosen to have a desired $f_{\max}$. The role of the term $f(d_{ij} - d_{ij}^*)\ {}^l x_j$ in (27) is to push agent i toward to or away from its neighbor j when the distance between them is larger or smaller than the desired distance, respectively.

From (27), the closed-loop dynamics in the global coordinate frame can be shown as

$$\dot{x} = Ax + F(x)x, \tag{28}$$

where A is the same as in (6), and $F : \mathbb{R}^{2n} \to \mathbb{R}^{2n \times 2n}$ is a $2n \times 2n$ matrix with similar Laplacian structure to A. In particular, $F(x)$ can be derived by replacing A_{ij} blocks in A by $f(d_{ij} - d_{ij}^*)I$, where I is the 2×2 identity matrix.

Clearly, the desired formation is an equilibrium of (28). Since f is bounded by $f_{\max}$, entries of $F(x)$ are bounded. Therefore, when distance from x to $\ker(\mathrm{A})$ is large, the dynamics due to the linear term Ax overpower the nonlinear dynamics $F(x)x$. In this case, $F(x)x$ can be treated as a perturbation in the nonzero elements of A, where by choosing $f_{\max}$ small, this perturbation can be made arbitrarily small. Therefore, trajectories are guaranteed to get arbitrarily close to $\ker(\mathrm{A})$. When x gets close to $\ker(\mathrm{A})$, Ax becomes small, and the nonlinear dynamics become dominant. Consequently, once agents are close to the desired shape, they slowly contract (or expand) to achieve the desired scale. We will not provide further analysis and the convergence to the desired formation under control (27) is left as a conjecture and will be a subject of future work.

V. Analysis

In this section we provide the proofs for the theorems discussed in Section IV.

A. Proof of Theorem 1

Proof. Matrices $\bar{A}_{rs}, r < s$ are the 2×2 matrix blocks in $\bar{A}$ that are above the diagonal. So the first constraint in (19) implies that $\bar{A}$ is a block lower triangular structure. Eigenvalues of a block lower triangular matrix are the eigenvalues of the diagonal blocks. Note that since control gains are restricted to the form (5), matrices $\bar{A}_{rs}$ inherit the same structure, i.e., in (18) we have $\bar{a}_{2r-1\ 2s-1} = \bar{a}_{2r\ 2s}$ and $\bar{a}_{2r-1\ 2s} = -\bar{a}_{2r\ 2s-1}$, for all $r,s \in \mathbb{N}_{n-2}$. Therefore, the eigenvalues of diagonal blocks $\bar{A}_{rr}$ are $\bar{a}_{2r\ 2s} \pm \imath\, \bar{a}_{2r-1\ 2s}$, where $\imath$ is the imaginary unit. Since $\bar{a}_{2r\ 2s} \leq -\varepsilon$ by the second constraint in (19), all eigenvalues of $\bar{A}$ have negative real parts. The last constraint in (19) implies that the desired formation is an equilibrium for the control (2). Note that from Lemma 3, $Ax^* = 0$ and $A\bar{x}^* = 0$ arise to the same set of constraints, and therefore the latter is redundant. With $\bar{A}$ being stable, convergence to the desired shape follows from Lemmas 4 and 5. Notice that since $\mathbf{1} \in \ker(A)$, the scale of the achieved shape can possibly be zero. Specifically, if all agents coincide initially, they remain that way through all time. □

B. Proof of Theorem 2

Proof. We examine the number of constraints that are imposed on control gains a_{ij}, b_{ij} by (19). Since 2×2 matrix blocks $\bar{A}_{rs}$ have the same structure as in (5), the condition for upper diagonal blocks to be zero imposes $(n-2)(n-3)$ linear constraints on control gains. The constraint $\operatorname{diag}(\bar{A}_{rr}) < -\varepsilon$, imposes $n-2$ linear constraints. Lastly, $Ax^* = 0$ imposes $2n$ linear constraints. The total number of constraints is therefore $(n-2)^2 + 2n$, and when $m \geq (n-2)^2 + 2n$, the number of linear constraints is less than or equal to the number of tunable gains. □

C. Proof of Theorem 3

Lemma 6. *If $\{\bar{A}^k \in \mathbb{C}^{n \times n} \,|\, k \in \mathbb{N}_K\}$ is a set of lower triangular stable matrices, then the switched linear system $\dot{y} = \bar{A}^{k(t)} y$ is globally uniformly exponentially stable (GUES) for any arbitrary switching (see Proposition 2.9 in [25]).*

Proof of Lemma 6 follows by observing that the stable lower triangular structure corresponds to the cascade connection of GUES systems. Entries of $\bar{A}^k$ can be complex. This implies that the block lower triangular matrices in which 2×2 blocks have the form (5) are GUES for any arbitrary switching.

Proof. Consider the set $\mathcal{G}$ of K sensing topologies, and denote the set of gain matrices by $\mathcal{A} := \{A^k \,|\, k \in \mathbb{N}_K\}$.

Assume $k(t) \in \mathbb{N}_K$ is an arbitrary switching signal for the dynamical system

$$\dot{x} = A^{k(t)} x, \quad A^{k(t)} \in \mathcal{A}. \tag{29}$$

Let $\mathcal{M} := \text{range}(N)$. Notice that $\mathcal{M}$ is an invariant manifold[10] for (29) since $\mathcal{M} \subset \ker(A^{k(t)})$. Further note that $Q^\top$ defined in (15) is the associated orthonormal projection matrix onto the orthogonal subspace $\mathcal{M}^\perp$. Consider the projected system

$$\begin{aligned} \dot{y} &= Q^\top A^{k(t)} Q y \\ &= \bar{A}^{k(t)} y. \end{aligned} \tag{30}$$

Note that (22) implies that all $\bar{A}^k$ matrices are block lower triangular and stable. Therefore, from Lemma 6 it follows that (30) is GUES. Since all trajectories of (30) exponentially converge to zero, all trajectories of (29) exponentially converge to $\mathcal{M}$. Thus, the desired shape is achieved. □

D. Proof of Theorem 4

Proof. We examine the number of linear constraints that are imposed by (22) on control gains. We showed in the proof of Theorem 2 that for a fixed topology, the block lower triangular structure of $\bar{A}$ imposes $(n-2)(n-3)$ constraints, and the negative diagonal condition imposes $n-2$ linear constraints on control gains. Similarly, for K different topologies, the block lower triangular structure of $\bar{A}^k, k \in \mathbb{N}_k$, imposes $K(n-2)(n-3)$, and negative diagonal condition imposes $K(n-2)$ linear constraints on control gains a_{ij}^k, b_{ij}^k. For the fixed topology, $Ax^* = 0$ imposed $2n$ constraints. The number of constraints imposed by $A^k x^* = 0$ is, however, generally less than $K(2n)$. This is because for topologies in which agents have identical neighbor sets, the associated rows of A^k are identical and therefore the constraints are redundant. Consequently, since S shows the total number of nonidentical neighbor sets for all agents in all topologies, the total number of constraints imposed by $A^k x^* = 0$ is $2S$. The total number of constraints is therefore $K(n-2)^2 + 2S$. The number of independent gains is m, where for agents that have the same neighbor set in different topologies the gains are counted only once. Therefore, when $m \geq K(n-2)^2 + 2S$, the number of constraints is less than or equal to the number of tunable gains. □

VI. Simulations

Consider four agents with the desired formation defined as a unit square. Assume that the sensing topology changes with time, and for simplicity is limited to undirected graphs. The set of all such topologies is shown in Fig. 3, for which control gains are designed via (26). Note that the choice of ε in (26) allows influence over the rate of convergence and here is chosen as 0.5.

One can verify that the conditions of Theorem 4 are met since $n = 4$, $K = 10$, $S = 16$, and $m = 72$. The gains found from (26) simultaneously stabilize all sensing topologies, and by Theorem 3, the desired shape is achieve under any arbitrary switching among topologies. The gains found via (26) are available to each agent, and at each instant of time, agents choose their control gains according to their current neighbor set.

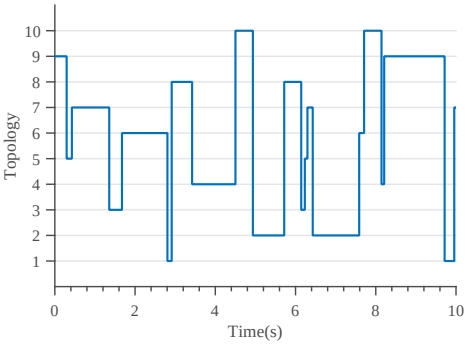

Fig. 4. Random switching among 10 sensing topologies given in Fig. 3.

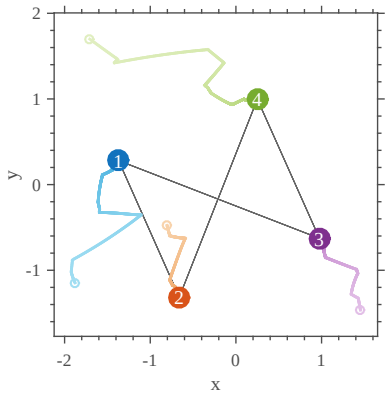

Fig. 5. Trajectories of four agents starting from a random initial position using control law (2). The sensing topology changes according to Fig. 4. The agents achieve the desired shape, which is defined as a square. Simulation video can be found at https://youtu.be/kwlzUAvGkS4 .

Figure 4 shows a randomly generated switching signal for topologies shown in Fig. 3. Under this switching scheme, Fig. 5 shows the trajectories of agents starting from a random initial position, where control (2) was used for the agents. Initial position of agents at $t = 0s$ is shown by circles, and final positions at $t = 10s$ are shown by discs in the figure. As can be seen from Fig. 4, the index of the sensing topology at $t = 10$ is 7, which coincides with the graph shown in Fig. 5 at the final time. Note that the scale of the formation achieved in Fig. 5 is not controlled, and depends on the starting position of the agents. Link to the simulation video is provided in the figure caption.

Under the same switching scheme, Fig. 6 shows trajectories of agents where control (27) was used for the agents. The control gains in (27) are the same as in (2), and map $f : \mathbb{R} \to \mathbb{R}$ is chosen as $f : z \mapsto \frac{1}{10}\arctan(z)$. The initial position of all agents is the same as in Fig. 5. As can be seen in Fig. 7, the distance error, defined as $e_{ij} := d_{ij} - d_{ij}^*$, goes to zero. Therefore, the agents achieve both the desired shape and scale, i.e., the desired formation. Link to the simulation video is provided in the figure caption.

[10] An invariant manifold $\mathcal{M}$ of a system $\dot{x} = f(x,t)$ is a manifold such that if $x(t_0) \in \mathcal{M}$, then $x(t > t_0) \in \mathcal{M}$.

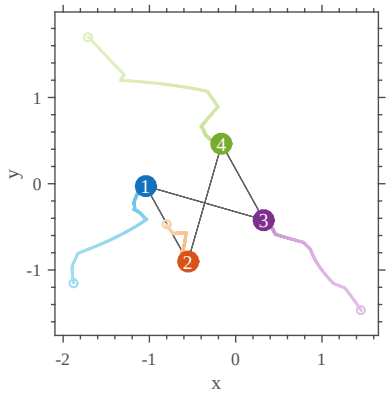

Fig. 6. Trajectories of four agents starting from a random initial position using the control law (27). The sensing topology changes according to Fig. 4. The agents achieve the desired formation, which is defined as a unit square. Simulation video can be found at https://youtu.be/vlTDORVGijI .

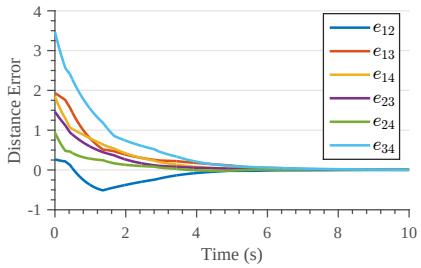

Fig. 7. Inter-agent distance error versus time. The error is defined as $e_{ij} := d_{ij} - d_{ij}^*$.

VII. Concluding Remarks and Future Work

We presented a distributed control scheme for a group of agents to autonomously achieve a desired geometric configuration. The desired configuration was defined in terms of inter-agent angles and distances, and only local relative position measurements were used to achieve this configuration. We designed the control for both fixed and changing sensing topologies, and provided the sufficient topological conditions that guarantee exponential convergence to the desired shape. The main contribution of this work was to prove that the sensing topology can change *arbitrarily*, and does *not* need to satisfy a dwell time constraint. Furthermore, agents did *not* need to communicate or have extra knowledge about the overall sensing topology.

To fix the scale of the achieved configuration to a desired value, we introduced the augmented control law (27), and started an initial discussion on its stability and convergence properties. Rigorous stability analysis for this control is a topic of future work. The stability requirements presented in Theorems 3 and 4 are only sufficient and may be conservative. It would be interesting to find the necessary conditions, for which the stability is ensured under the minimum topological requirements. Lastly, to enjoy the simplifications that arise from the commutativity property, the control gains where restricted to the form (5), where two degrees of freedom were lost. One can expect the extra degrees of freedom to improve the control performance. Therefore, exploring the design techniques without restricting the gain matrices is worthwhile.

References

[1] D. Pickem, L. Wang, P. Glotfelter, Y. Diaz-Mercado, M. Mote, A. Ames, E. Feron, and M. Egerstedt, "Safe, remote-access swarm robotics research on the robotarium," *arXiv preprint arXiv:1604.00640*, 2016.

[2] R. Tron, J. Thomas, G. Loianno, K. Daniilidis, and V. Kumar, "A distributed optimization framework for localization and formation control: Applications to vision-based measurements," *IEEE Control Systems*, vol. 36, no. 4, pp. 22–44, Aug 2016.

[3] M. Whitzer, J. Keller, S. Bhattacharya, V. Kumar, T. Sands, L. Ritholtz, A. Pope, and D. Dickmann, "In-flight formation control for a team of fixed-wing aerial vehicles," in *International Conference on Unmanned Aircraft Systems*. IEEE, 2016, pp. 372–380.

[4] J. C. Zegers, E. Semsar-Kazerooni, J. Ploeg, N. van de Wouw, and H. Nijmeijer, "Consensus-based bi-directional CACC for vehicular platooning," in *2016 American Control Conference*. IEEE, 2016, pp. 2578–2584.

[5] L. Y. Wang, A. Syed, G. G. Yin, A. Pandya, and H. Zhang, "Control of vehicle platoons for highway safety and efficient utility: Consensus with communications and vehicle dynamics," *Journal of systems science and complexity*, vol. 27, no. 4, pp. 605–631, 2014.

[6] J. Seo, M. Yim, and V. Kumar, "Assembly sequence planning for constructing planar structures with rectangular modules," in *IEEE International Conference on Robotics and Automation*, 2016, pp. 5477–5482.

[7] A. Spröwitz, R. Moeckel, M. Vespignani, S. Bonardi, and A. J. Ijspeert, "Roombots: A hardware perspective on 3D self-reconfiguration and locomotion with a homogeneous modular robot," *Robotics and Autonomous Systems*, vol. 62, no. 7, pp. 1016–1033, 2014.

[8] R. Olfati-Saber and R. M. Murray, "Distributed cooperative control of multiple vehicle formations using structural potential functions," in *IFAC World Congress*, 2002, pp. 346–352.

[9] L. Krick, M. E. Broucke, and B. A. Francis, "Stabilisation of infinitesimally rigid formations of multi-robot networks," *International Journal of Control*, vol. 82, no. 3, pp. 423–439, 2009.

[10] Y.-P. Tian and Q. Wang, "Global stabilization of rigid formations in the plane," *Automatica*, vol. 49, no. 5, pp. 1436–1441, 2013.

[11] M. Basiri, A. N. Bishop, and P. Jensfelt, "Distributed control of triangular formations with angle-only constraints," *Systems & Control Letters*, vol. 59, no. 2, pp. 147–154, 2010.

[12] M. H. Trinh, K.-K. Oh, and H.-S. Ahn, "Angle-based control of directed acyclic formations with three-leaders," in *International conference on mechatronics and control*, 2014, pp. 2268–2271.

[13] M. Deghat and A. N. Bishop, "Distributed shape control and collision avoidance for multi-agent systems with bearing-only constraints," in *European Control Conference*. IEEE, 2015, pp. 2342–2347.

[14] S. Zhao and D. Zelazo, "Bearing rigidity and almost global bearing-only formation stabilization," *IEEE Transactions on Automatic Control*, vol. PP, no. 99, pp. 1–1, 2015.

[15] Z. Lin, L. Wang, Z. Chen, M. Fu, and Z. Han, "Necessary and sufficient graphical conditions for affine formation control," *IEEE Transactions on Automatic Control*, 2014.

[16] A. N. Bishop, T. H. Summers, and B. D. Anderson, "Stabilization of stiff formations with a mix of direction and distance constraints," in *IEEE International Conference on Control Applications*, 2013, pp. 1194–1199.

[17] A. N. Bishop, M. Deghat, B. Anderson, and Y. Hong, "Distributed formation control with relaxed motion requirements," *International Journal of Robust and Nonlinear Control*, 2014.

[18] K. Fathian, D. I. Rachinskii, M. W. Spong, and N. R. Gans, "Globally asymptotically stable distributed control for distance and bearing based multi-agent formations," in *2016 American Control Conference*. IEEE, 2016, pp. 4642–4648.

[19] K. Fathian, D. I. Rachinskii, T. H. Summers, and N. R. Gans, "Distributed control of cyclic formations with local relative position measurements," *to appear, IEEE Conference on Decision and Control*, 2016.

[20] Z. Lin, L. Wang, Z. Han, and M. Fu, "Distributed formation control of multi-agent systems using complex laplacian," *IEEE Transactions on Automatic Control*, vol. 59, no. 7, pp. 1765–1777, July 2014.

[21] ——, "A graph laplacian approach to coordinate-free formation stabilization for directed networks," *IEEE Transactions on Automatic Control*, vol. 61, no. 5, pp. 1269–1280, May 2016.

[22] T. Han, R. Zheng, Z. Lin, and M. Fu, "A barycentric coordinate based approach to formation control of multi-agent systems under directed and switching topologies," in *IEEE Conference on Decision and Control*, 2015, pp. 6263–6268.

[23] L. Wang, Z. Han, and Z. Lin, "Realizability of similar formation and local control of directed multi-agent networks in discrete-time," in *IEEE Conference on Decision and Control*, 2013, pp. 6037–6042.

[24] M. Grant and S. Boyd, "CVX: Matlab software for disciplined convex programming, version 2.1," http://cvxr.com/cvx, Mar. 2014.

[25] D. Liberzon, *Switching in systems and control*. Springer Science & Business Media, 2012.